Bose-Fermi mixtures in 1D few-sites optical lattices

Gerard Pelegrí Andrés
*Facultat de Física, Universitat de Barcelona, Diagonal 645, 08028 Barcelona, Spain.**

Advisors: Bruno Juliá-Díaz and Artur Polls.

We use exact diagonalization techniques to study the ground state properties of few-site optical lattices where bosons and fermions are mixed and interact. First, we consider a two-site system with 50 bosons and one single fermionic impurity. The interaction of the impurity with the bosonic background is shown to modify its properties. Then, we consider a three-site system in order to see effects of the fermionic nature of the impurities. In this system, the modification of the properties of the bosons by the interaction with the fermions is even more dramatic, and is different when the system hosts one fermion than two.

I. INTRODUCTION

In recent years, it has become experimentally possible to confine ultracold atomic systems in optical lattices [1, 2]. Such lattices are created with standing laser beams and consist of periodic electromagnetic potentials. The atoms that see this potential can occupy any of its minima, and since they also have kinetic energy, hoping between adjacent potential minima is possible. If the atoms are of bosonic type, there can be any number of them in each potential minimum and on-site interactions have to be taken into account.

Ultracold atomic systems in optical lattices allow a high control of all the relevant parameters. By modifying the configuration of the lasers, it is possible to create lattices in one, two or three dimensions with virtually any desired periodicity. Tuning the lasers also allows to control the depth of the potential minima and thus enhance or difficult the hoping of the atoms. Furthermore, using Feshbach resonances [3] one can vary the s-wave scattering length of the atoms in a wide range of negative and positive values, which means that the on-site interatomic interactions can be controlled to be attractive or repulsive and to have any desired strength. This high level of control, together with the many analogies that exist between ultracold atoms in optical lattices and a number of other quantum systems that are much less experimentally accessible [4], has awaken a huge interest for ultracold atoms in optical lattices not only because of their singular mesoscopic quantum properties, but also as quantum simulators.

Systems of few bosons and fermions have been studied [5–9]. Also, Bose-Fermi mixtures have been studied from different approaches [10–13]. The aim of this work is to perform a numerical study of the properties of mixtures of bosonic and fermionic spinless atoms in few sites, one-dimensional optical lattices. For such purpose, we will model the lattice as a collection of sites and use a Bose-Fermi-Hubbard Hamiltonian in second quantization to describe the system

$$\hat{\mathcal{H}} = -J_b \sum_i (\hat{a}_i^\dagger \hat{a}_{i+1} + \hat{a}_{i+1}^\dagger \hat{a}_i) - J_f \sum_i (\hat{b}_i^\dagger \hat{b}_{i+1} + \hat{b}_{i+1}^\dagger \hat{b}_i) + \frac{U_{bb}}{2} \sum_i \left[\hat{a}_i^\dagger \hat{a}_i (\hat{a}_i^\dagger \hat{a}_i - 1)\right] + U_{bf} \sum_i \hat{a}_i^\dagger \hat{a}_i \hat{b}_i^\dagger \hat{b}_i, \quad (1)$$

where a_i and b_i are the destruction operators of a boson and a fermion in the site i, which satisfy the relations

$$[\hat{a}_i, \hat{a}_j] = 0; \quad [\hat{a}_i^\dagger, \hat{a}_j^\dagger] = 0; \quad [\hat{a}_i, \hat{a}_j^\dagger] = \delta_{ij} \quad (2)$$

$$\{\hat{b}_i, \hat{b}_j\} = 0; \quad \{\hat{b}_i^\dagger, \hat{b}_j^\dagger\} = 0; \quad \{\hat{b}_i, \hat{b}_j^\dagger\} = \delta_{ij} \quad (3)$$

$$[\hat{a}_i, \hat{b}_j] = 0; \quad [\hat{a}_i^\dagger, \hat{b}_j^\dagger] = 0; \quad [\hat{a}_i, \hat{b}_j^\dagger] = 0. \quad (4)$$

The first two terms in (1) account for the hoping (kinetic energy) of bosons and fermions. The other two terms account for the on-site interactions: the third one is the interaction of all the possible bosonic pairs in each site and the last term contains the interaction of all the bosons in one site with the fermion in that site (because of the Pauli principle, there can be only one or zero fermions in each site). Since there is a high experimental level of control over the tunnelling and the on-site interactions, it will be realistic to vary the constants J_b, J_f, U_{bb} and U_{bf} to explore different regimes of the system.

In general, we will use the following procedure to perform our numerical studies

1. Identify the system that we want to describe: how many sites it has, what is their topology and how many bosons and fermions are placed on them.
2. Build a Fock basis of the whole Hilbert space associated to the system.
3. Compute the matrix elements of $\hat{\mathcal{H}}$ in such Fock basis and use numerical diagonalization techniques to find its eigenstates and their eigenenergies.

We will consider two basic kinds of systems. First, we will focus on a two-site system with 50 bosons and 1 fermion that can interact attractively or repulsively. Although this is a good starting point for our purposes, having only 1 fermion is equivalent to having 1 boson of another type

*Electronic address: gerard.pelegri@gmail.com

(impurity), and thus it is not possible to see any quantum statistical effect. In order to see this kind of effect, we will later consider a system of 3 sites with periodic boundary conditions filled with 12 bosons and 0,1 or 2 fermions.

II. TWO-SITE SYSTEM WITH A SINGLE (FERMIONIC) IMPURITY

The first system that we shall consider consists of two sites that are filled with $N_b = 50$ bosons and 1 fermion. The natural Fock basis that describes all the possible states in this system is

$$\{|k, N_b - k; 0, 1\rangle, |k, N_b - k; 1, 0\rangle\}; \quad k = 0, 1, 2, ..., N_b$$

i.e., the Hilbert space has size $2(N_b + 1)$, with the first $N_b + 1$ states corresponding to all the possible bosonic configurations with the fermion in the right site and the second half of the Fock states corresponding to all the possible bosonic configuration with the boson in the left site.

In our study of this system, we will assume for the constants in (1) $J_b = J_f = 1$ and $|U_{bb}| = |U_{bf}| \equiv U$. Rather than the specific values of all the energy constants, the parameter which is more relevant for the properties of the system is the interaction strength, i.e., ratio between the total on-site interaction and the tunnelling energy, $\Lambda = \frac{N_b U}{J}$. When diagonalizing the system for high values of Λ, the quasi-degeneracy of the states can cause numerical instabilities that break the symmetry of the system choosing arbitrarily any of the sites. A way to avoid this problem is to introduce a little bias in (1) that breaks the symmetry artificially in a site of our choice. Thus, our Hamiltonian for this model will be

$$\hat{\mathcal{H}}^{(2)} = \hat{\mathcal{H}} - \epsilon(\hat{a}_1^\dagger \hat{a}_1 - \hat{a}_2^\dagger \hat{a}_2), \tag{5}$$

with $\epsilon = 10^{-7}$.

A. Static properties

A general many-body eigenstate of the Hamiltonian (5) will be written as $|\Psi\rangle = \sum_k c_k^r |k, N_b - k; 0, 1\rangle + c_k^l |k, N_b - k; 1, 0\rangle$. In Fig. 1 we plot the spectral decomposition of the ground and highest excited state for the system with both boson-boson and boson-fermion attractive interaction and different values of Λ. The spectral decomposition of the two-site system with $N_b = 50$ bosons and no fermion, computed in [14], is also plotted for comparison. As can be seen in Fig. 1, for low values of the interaction strength ($\Lambda = 1$) the most populated Fock states in both the ground and highest excited states of the system without fermion are those with approximately equal number of bosons in both sites. This is also the case in the system with one fermionic impurity, but with a symmetry between the states with the fermion in each site. As the interaction strength is increased ($\Lambda = 3$), the ground state of the system with no fermion becomes cat-like: there is equal probability to find all the bosons in either of the two sites. The ground state of the system with a fermion adopts a similar form, but since there is an attractive boson-fermion interaction it is more likely to find the system in a state in which the bosons are concentrated in one site and the fermion is in the same site. The left-right fermionic symmetry is still conserved. Finally, when the interaction is increased further ($\Lambda = 7$), the bias term breaks the symmetry in both the purely bosonic system and the system with an impurity.

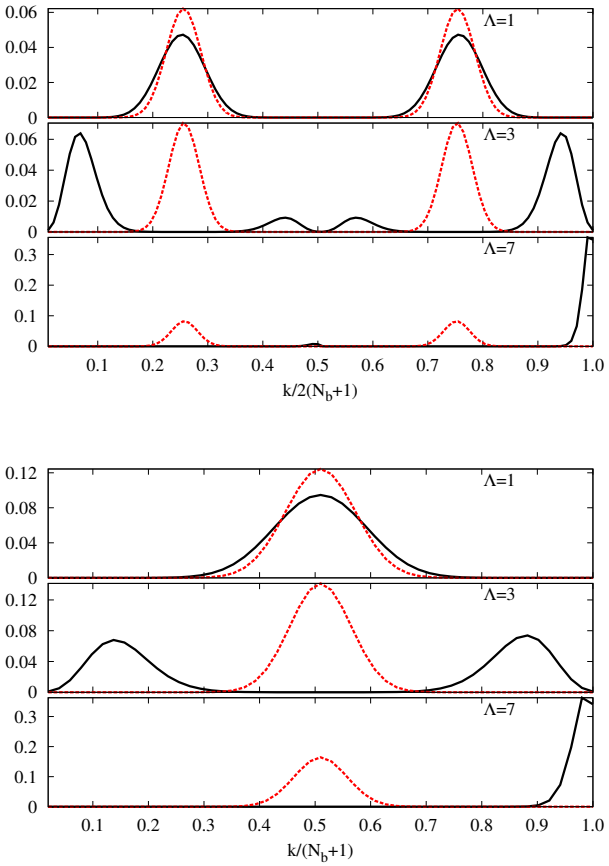

FIG. 1: Spectral decomposition $|c_k|^2$ of the ground (black, solid) and highest excited state (red, dashed) of the system with two sites, $N_b = 50$ and 1 fermion (top panels) and the system with two sites and $N_b = 50$ bosons (bottom panels) for different values of Λ. All interactions are attractive; under an exchange of the sign of the interaction the ground and highest excited state would exchange their roles.

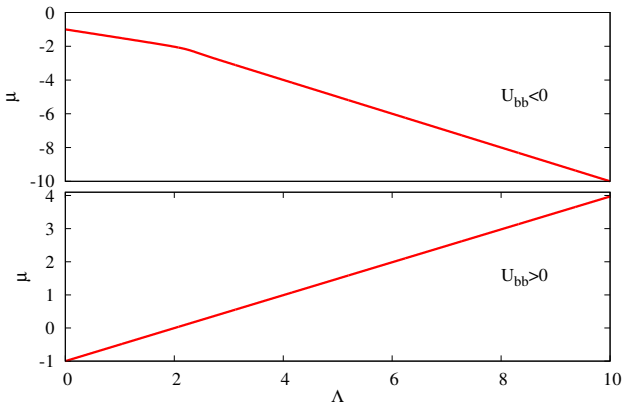

FIG. 2: Chemical potential of the system of two sites with 50 bosons and 1 fermion as a function of the strength Λ. The top and bottom panels correspond to attractive and repulsive boson-boson interaction respectively.

Chemical potential and transition to the cat-like ground state

A quantity that can be studied to determine at which value of the interaction strength the spectral decomposition of the ground state stops being centered around the Fock states with equal number of bosons in each site is the chemical potential μ, which is defined as the change of the energy of the ground state after removing one particle. In our system, we will assume that the particle that we remove is a boson (under the condition $|U_{bb}| = |U_{bf}|$, removing a boson or the fermion yields the same results), so that the chemical potential is defined as

$$\mu = E_0(N_b) - E_0(N_b - 1). \tag{6}$$

As can be seen in Fig. 1, for $U_{bb} < 0$, at low values of Λ the spectral decomposition of the ground state is centered around the Fock states with equal number of bosons in each site, $|N_b/2, N_b/2\rangle$. Not taking into account the tunnelling term in (1), the energy of this ground state is $E_0(N_b) \sim \frac{U_{bb}}{2} 2 \cdot \frac{N_b}{2}(\frac{N_b}{2} - 1)$. When removing a boson, the ground state becomes centred around bosonic configurations close to $|N_b/2, N_b/2 - 1\rangle$, so its energy is $E_0(N_b - 1) \sim \frac{U_{bb}}{2}\left(\frac{N_b}{2}(\frac{N_b}{2} - 1) + (\frac{N_b}{2} - 1)(\frac{N_b}{2} - 2)\right)$. Thus, in this regime $E_0(N_b) - E_0(N_b - 1) \sim \frac{N_b U_{bb}}{2}$. However, as it can also be seen in Fig. 1, for higher values of Λ the spectral decomposition of the ground state becomes peaked at Fock states with different number of bosons in each site. It is not necessary to set very high values of the interaction so that this ground state has bosonic configurations of the type $|N_b, 0\rangle$, and thus an energy (without tunnelling term) $E_0(N_b) \sim \frac{U_{bb}}{2} N_b(N_b - 1)$, and so the difference of energies after removing one boson is $E_0(N_b) - E_0(N_b - 1) \sim U_{bb} N_b$. In the case of repulsive boson-boson interaction, the ground state interchanges its role with the highest excited state in Fig. 1, so that in this case the ground state is always peaked around Fock states with equal number of bosons in both sites and $E_0(N_b) - E_0(N_b - 1) \sim \frac{U_{bb} N_b}{2}$.

These simple considerations allow to explain the chemical potential curves shown in Fig. 2 for $U_{bb} < 0$ and $U_{bb} > 0$. In both cases, the chemical potential curves start at $\mu(\Lambda = 0) = -1$, because in the absence of interaction the only energetic difference between the system of N_b and $N_b - 1$ bosons is the tunnelling energy of one boson. In the attractive case, for low values of the interaction the slope of the chemical potential is initially $-\frac{1}{2}$, which is consistent with the considerations made above if we recall that $\Lambda = \frac{NU}{J}$ and we take into account that in this case $U_{bb} < 0$ and that we have set $J = 1$. Then, at $\Lambda \approx 2$ the slope changes to -1, and this change is associated with the transition to the regime where the ground state is cat-like. As expected, in the case of repulsive boson-boson interaction the slope of the chemical potential is constant and equal to $\frac{1}{2}$. However, at the same value of Λ for which there is the change of slope in the attractive case, the chemical potential vanishes. This value of the interaction, for which it costs no energy to remove one particle from the system, can be regarded as the interaction strength which equates the importance of the tunnelling and the on-site interactions, so it makes sense that it is the same strength for which there is the change of slope when $U_{bb} < 0$.

Population imbalance and effect of the bias

The study of the population imbalance of the ground state can be used to determine at which value of the interaction strength the bias term in the Hamiltonian breaks the symmetry by selecting one of the sites. The population imbalance is defined as the difference between the bosonic/fermionic populations of the two sites

$$\hat{z} = \frac{\hat{n}_1 - \hat{n}_2}{N}. \tag{7}$$

If the symmetry between the two sites is preserved, the population imbalance will be zero both for bosons and the fermionic impurity, and when the bias selects one site it will acquire a non-zero value that should increase with Λ. In Fig. 3 it can be seen that the imbalance of both the bosons and the fermion remains $z = 0$ as the interaction strength is increased, until a critical value $\Lambda \approx 3$ at which they increase abruptly to 1 (the bias selects the site 1 in front of 2). The dispersion of the bosonic population imbalance increases softly in the region where the spectral decomposition of the ground state is peaked around the Fock states with equal number of bosons in each site ($0 < \Lambda < 2$) due to the broadening that occurs when the interaction strength is increased. Then, in the region $2 < \Lambda < 3$ it increases more sharply because the ground state is cat-like and the peaks in the spectral decomposition go further and further apart when the interaction strength is increased. In the region where the bias selects

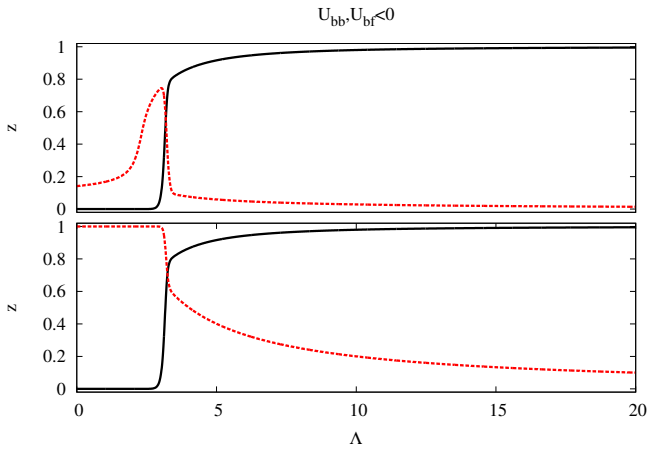

FIG. 3: Expectation value of the population imbalance of the ground state $z = \langle\phi_0|\hat{z}|\phi_0\rangle$ (black, solid) and its dispersion (red, dashed) $\Delta z = \sqrt{\langle\hat{z}^2\rangle - \langle\hat{z}\rangle^2}$ of the bosons (top) and the fermion (bottom) as a function of the interaction strength for both boson-boson and boson-fermion attractive interactions. N_b is 50.

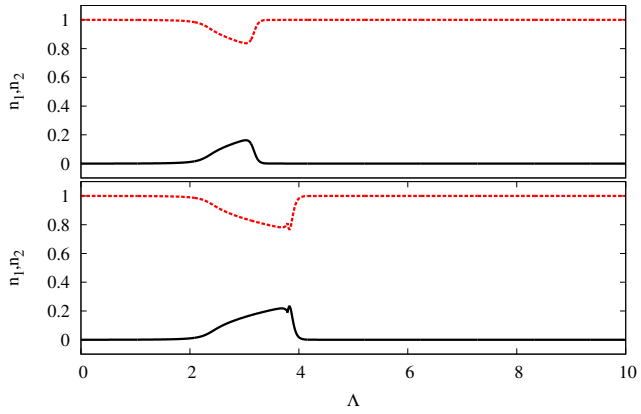

FIG. 4: Eigenvalues of the one body density matrix (divided by $N_b = 50$) of the bosons as a function of the interaction strength for the system with one fermionic impurity (top) and the system without fermion (bottom) for all interactions attractive.

the site 1, the dispersion in the bosonic population imbalance goes rapidly to 0. As for the fermion, the dispersion in its population imbalance is 1 until the bias selects the site 1: because of the symmetry it is equally probable to find the fermion in either of the two sites. When the bias starts playing a role, the dispersion in the fermionic imbalance goes to zero, but it does less rapidly than in the case of the bosons because of the statistical effect that there is only one fermion in front of 50 bosons.

One-body density matrix and condensed fraction

As it is well known, ultracold bosonic systems may form a Bose-Einstein condensate, in which all bosons occupy the same quantum state and behave coherently. In our system, a quantity that can be used to study the condensed fraction of the bosons is the one body density matrix of the ground state $|\phi_0\rangle$, defined as

$$\rho_{ij} = \langle\phi_0|\hat{a}_i^\dagger\hat{a}_j|\phi_0\rangle\,. \tag{8}$$

The trace of this matrix is normalized to the total number of bosons in the system. When diagonalizing it, the presence of an eigenvalue equal to the total number of particles indicates that the bosons are totally condensed, i.e., the total many-body state can be written as a product of N_b identical single particle states. In Fig. 4 the eigenvalues of the one body density matrix as a function of the interaction strength for the system without fermionic impurity and our system are plotted. The range of interaction strengths for which there is no total condensation ($n_1 \neq 1$) is slightly broader in the system without fermion. Thus, the presence of an impurity slightly enhances the condensation of the bosons.

B. Dynamic evolution

Once one has diagonalized the system and determined all its eigenstates $\{\phi_i\}$ and spectrum $\{E_i\}$, it is possible to find the time evolution of an initial state $|\Psi\rangle$ by simply projecting it to the basis of eigenstates

$$|\Psi\rangle\,(t) = \sum_{i=1}^{2(N_b+1)} e^{-\frac{iE_i t}{\hbar}}\,\langle\phi_i|\Psi\rangle\,|\phi_i\rangle\,. \tag{9}$$

A choice for the initial state of the system that may be experimentally accessible is a single Fock state in which all the bosons are concentrated in one site and the fermion is in the same site, for instance $|\Psi\rangle = |N_b, 0; 1, 0\rangle$. We set attractive boson-boson interaction and repulsive boson-fermion interaction (the results do not depend on the sign of this interaction) and study the time evolution of the bosonic population imbalance and of the probability of finding the fermion in each of the two sites for different values of the interaction strength Λ. In Fig. 5 one can see that as the interaction strength is increased, the system becomes self-trapped: at $\Lambda = 3$, the probabilities of finding the fermion in either of the two sites oscillate and for a long period of time it is equally likely to find the fermion in any of the two sites. At this value of the strength, the population imbalance undergoes big oscillations as well, which means that the bosons are not localized. However, at $\Lambda = 10$ the probability of finding the fermion in site 1 does not oscillate very far from its initial value of 1, and the bosonic population imbalance has a similar behavior. Interestingly, as it can be seen in the lowest panel of Fig. 5, the probability of finding the fermion in site 1 and the population imbalance oscillate in phase, which indicates that there is also a dynamic correlation of the fermion with the boson due to the interaction.

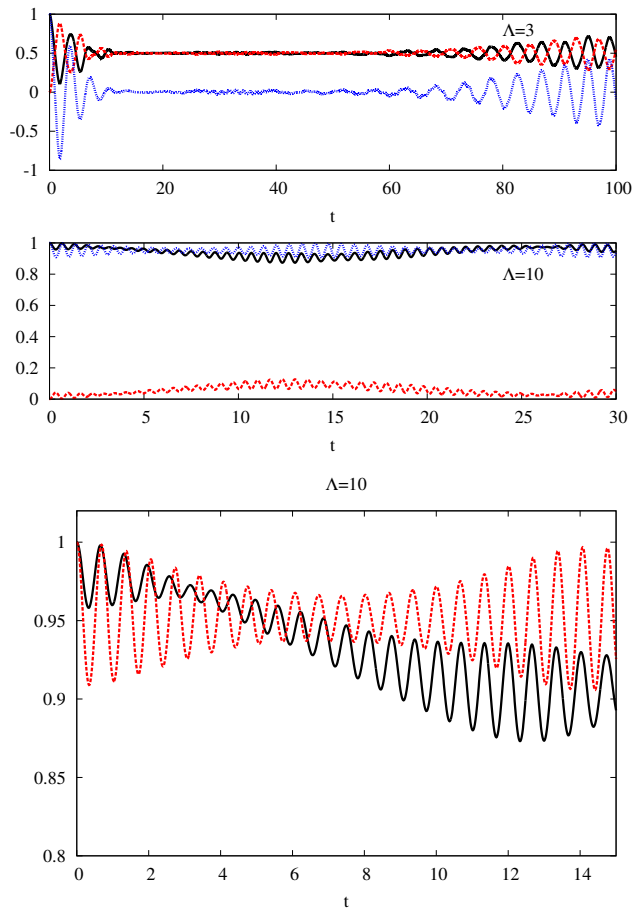

FIG. 5: Initial state: $|N_b, 0; 1, 0\rangle$. First two panels: time evolution of the probabilities of finding the fermion in site 1 (black, solid), in site 2 (red, line-dashed) and of the bosonic population imbalance (blue, dot-dashed) for $U_{bb} < 0$ and different values of Λ. In the lowest panel the population imbalance (red, dot-dashed) and the probability of finding the fermion in site 1 (black, solid) are plotted simultaneously in a shorter time range for $\Lambda = 10$. N_b is 50.

III. THREE-SITE SYSTEM

So far, we have considered a system of two sites filled with N_b bosons and 1 fermion, where we have shown that the interaction of the fermion with the bosons modifies the properties of the latter. However, in this system it is not possible to see any specific effect of the different quantum statistics of the fermion, for we could also have regarded the fermion as a bosonic impurity distinguishable from the other N_b bosons.

In this section we shall consider a one-dimensional lattice of 3 sites, which is the minimum system in which the Pauli principle allows to place more than one mobile fermion and thus see some specific effect of the Fermi-Dirac statistics. We shall set periodic boundary conditions for the system: hoping between sites 1 and 3 is also possible (triangle topology), and we shall place 0, 1 or 2 fermions in it. The size of the bosonic Hilbert subspace of this system is $\frac{(N_b+2)!}{2!N_b!}$. The dimension of the bosonic subsystem increases very rapidly with the number of bosons, and in order not to exceed our computational capacity we have set a total number of $N_b = 12$ bosons in the system, for which there are 91 possible Fock states. As for the fermions, the size of their Hilbert space is $\frac{3!}{N_f!(3-N_f)!}$, so that the total size of the system will be $91 \times 1 = 91$ for $N_f = 0$ and $91 \times 3 = 273$ for $N_f = 1, 2$. The suitable Fock basis to describe all the possible states of the system, for $N_f = 0, 1, 2$, are,

$$\{|k_1, k_2, N_b - (k_1 + k_2)\rangle\}$$
$$\{|k_1, k_2, N_b - (k_1 + k_2)\rangle \otimes (|0, 0, 1\rangle + |0, 1, 0\rangle + |1, 0, 0\rangle)\}$$
$$\{|k_1, k_2, N_b - (k_1 + k_2)\rangle \otimes (|1, 1, 0\rangle + |1, 0, 1\rangle + |0, 1, 1\rangle)\},$$

with $k_1, k_2 = 0, 1, ..., N_b$ and $N_b - (k_1 + k_2) \geq 0$. The tunnelling constants in our model Hamiltonian (1) will be $J_b = J_f = 1$ as in the previous two-site model. This time however, we will allow the boson-boson and boson-fermion interaction constants to have different absolute values, and for this reason we introduce a new parameter $\Delta = \frac{|U_{bf}|}{|U_{bb}|}$. The reference interaction to define the interaction strength will be the boson-boson interaction, which in our studies will always be positive $U_{bb} = \frac{\Lambda J}{N_b}$ ($\Lambda > 0$). The boson-fermion interaction will be taken attractive, so that as a function of all the other parameters will be defined as $U_{bf} = -\frac{\Delta \Lambda J}{N_b}$. In some cases, there will be quasi-degeneracies in the spectrum that would induce numerical instabilities. In order to avoid this problem, we introduce again a bias, this time both for fermions and bosons, that selects sites by order of preference 1,2,3. Thus, the final Hamiltonian for this system reads

$$\hat{\mathcal{H}}^{(3)} = \hat{\mathcal{H}} - \epsilon(\hat{a}_1^\dagger \hat{a}_1 + \hat{b}_1^\dagger \hat{b}_1 - \hat{a}_3^\dagger \hat{a}_3 - \hat{b}_3^\dagger \hat{b}_3), \qquad (10)$$

with $\epsilon = 10^{-7}$.

A. System with no fermions

In order to understand better the results corresponding to having 1 and 2 fermions in the system, we first perform some calculations for the system with no fermions and $N_b = 12$ bosons, with $U_{bb} > 0$. We start by plotting in Fig. 6 the spectral decomposition of the ground state, which is written in general as $|\phi_0\rangle = \sum_{k_1,k_2} c(k_1, k_2) |k_1, k_2, N_b - (k_1 + k_2)\rangle$. At zero interaction, the ground state is analytical and can be written as a multinomial expansion

$$|\phi_0\rangle_{\Lambda=0} = \frac{1}{\sqrt{N_b!}} \left(\frac{\hat{a}_1^\dagger + \hat{a}_2^\dagger + \hat{a}_3^\dagger}{\sqrt{3}} \right)^{N_b} |\text{vac}\rangle$$
$$= \frac{1}{\sqrt{3^{N_b} N_b!}} \sum_{i,j,k}^{i+j+k=N_b} \frac{N_b!}{i!j!k!} (\hat{a}_1^\dagger)^i (\hat{a}_2^\dagger)^j (\hat{a}_3^\dagger)^j |\text{vac}\rangle . \qquad (11)$$

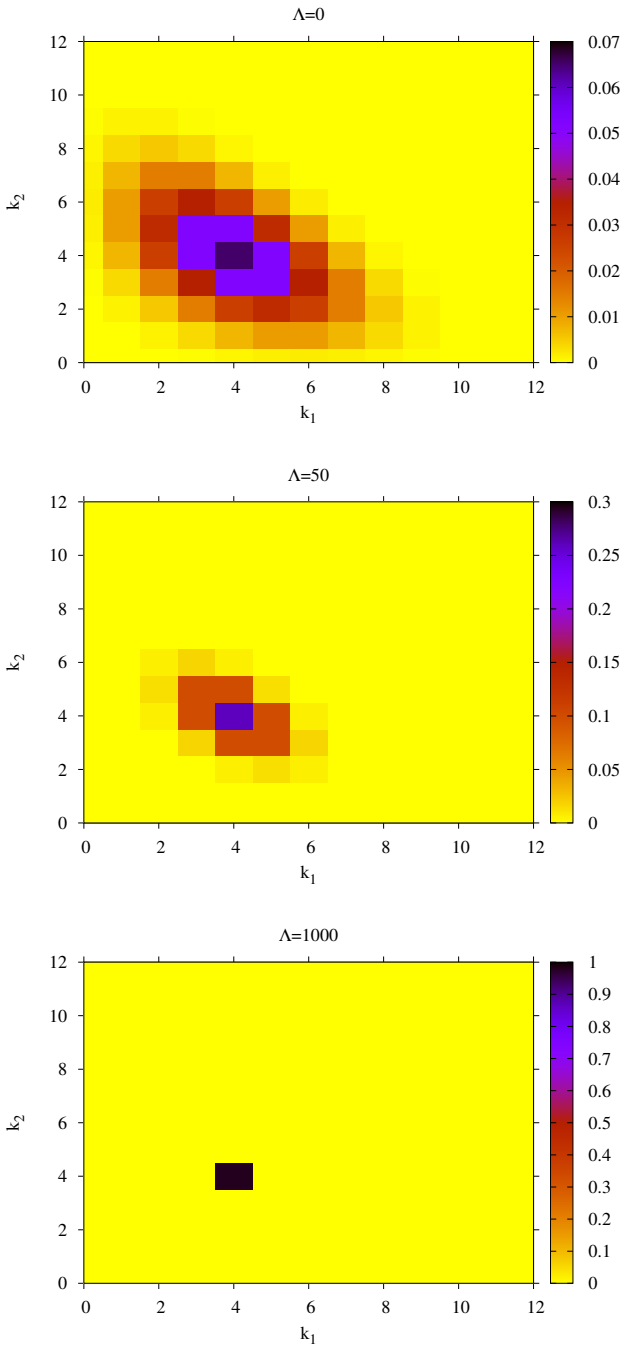

FIG. 6: Spectral decomposition of the ground state for different values of Λ. The color map corresponds to the probability $|c(k_1, k_2)|^2$ of the Fock states.

The zero interaction profile shown in Fig. 6 coincides with the one obtained with the analytical expression (11). As Λ is increased, the spectral decomposition of the ground state becomes more and more peaked around a reduced number of Fock states, and eventually around only one of such states.

The states around which the ground state becomes more and more peaked are those with the lowest expectation value of the Hamiltonian, which in our case of repulsive boson-boson interaction is given by

$$\frac{\langle n_1, n_2, n_3|\hat{\mathcal{H}}|n_1, n_2, n_3\rangle}{U_{bb}} = \frac{1}{2}\left(n_1(n_1-1) + n_2(n_2-1) + n_3(n_3-1)\right). \quad (12)$$

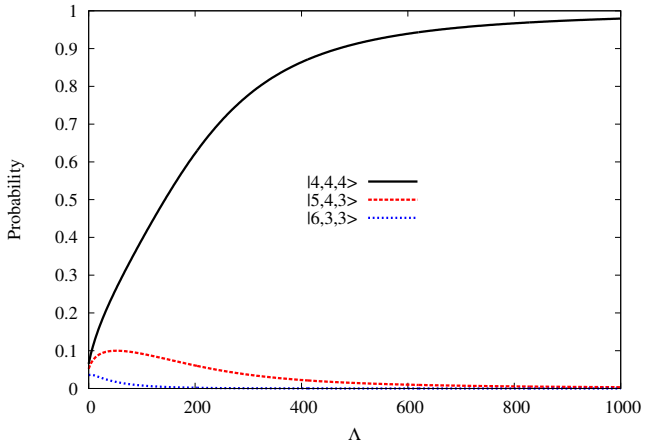

FIG. 7: Population of the lowest energy Fock states in the ground state as a function of the interaction strength. The states with the bosonic occupations n_1, n_2, n_3 permuted in the different sites have the same expectation values of the Hamiltonian, so only one Fock state of each family is plotted.

In Fig. 7 we plot the probability of finding the ground state in the Fock states with a lowest expectation value of the Hamiltonian (12) as a function of the interaction strength. As Λ is increased from 0, the lowest energetic Fock state $|4, 4, 4\rangle$ and the family of second lowest energetic Fock states $\{|5, 4, 3\rangle\}$ become more populated. In the strongly interacting limit, the tunnelling term of the Hamiltonian can be neglected and the ground state coincides essentially with the Mott-insulator Fock state $|4, 4, 4\rangle$.

As can be seen in Fig. 8, the system is only fully condensed in the non-interacting case, when the ground state of the system is the mean-field state (11). As the interaction strength is increased and the ground state approaches the Mott-insulator state, the three eigenvalues of the one-body density matrix tend to 4, as can be seen in Fig. 8.

B. Systems with one and two fermions

After studying the properties of the three-site system in the simpler case when there are no fermions, we shall focus on the properties of the one and two-fermion three-site systems. As we shall proof next, there is a direct correspondence between these two systems, and so it makes sense to discuss both of them at the same time.

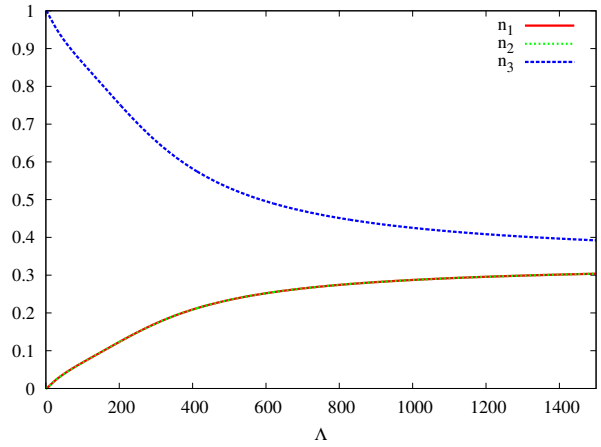

FIG. 8: Eigenvalues (divided by $N_b = 12$) of the one-body density matrix of the system with no fermions as function of Λ.

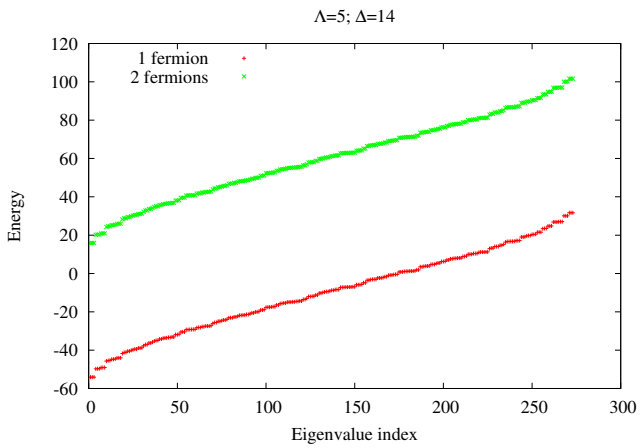

FIG. 9: Comparison of the spectrum of the system with one fermion ($U_{bf} < 0$) and the system with two fermions ($U_{bf} > 0$) for the same values of Λ and Δ. The two spectra have exactly the same shape but with a shift $N_b U_{bf} = \frac{\Delta\Lambda}{J}$.

Let us show that under an exchange of the sign of the boson-fermion interaction the one-fermion and the two-fermion (one hole) system are equivalent, i.e., the system with one fermion and $U_{bf} < 0$ is equivalent to that with two fermions and $U_{bf} > 0$; and the system with one fermion and $U_{bf} > 0$ is equivalent to that with two fermions and $U_{bf} < 0$.

Consider our model Hamiltonian $\hat{\mathcal{H}}$ (see (1)) and an eigenstate of the system with one fermion

$$|\Psi\rangle = \sum_{n_1,n_2,n_3\equiv j} a_j^1 \,|j;0,0,1\rangle + a_j^2 \,|j;0,1,0\rangle + a_j^3 \,|j;1,0,0\rangle \tag{13}$$

$$\hat{\mathcal{H}}\,|\Psi\rangle = E\,|\Psi\rangle\,. \tag{14}$$

Then, a state $|\Psi\rangle'$ of the system with two fermions which has the same form as $|\Psi\rangle$ but with a hole instead of a fermion,

$$|\Psi\rangle' = \sum_{n_1,n_2,n_3\equiv j} a_j^1 \,|j;1,1,0\rangle + a_j^2 \,|j;1,0,1\rangle + a_j^3 \,|j;0,1,1\rangle\,, \tag{15}$$

is an eigenstate of a Hamiltonian $\hat{\mathcal{H}}'$ with the same coefficients as $\hat{\mathcal{H}}$ except for a change of sign in the boson-fermion interaction $U_{bf} \to -U_{bf}$

$$\hat{\mathcal{H}}'\,|\Psi\rangle' = (E - N_b U_{bf})\,|\Psi\rangle'\,. \tag{16}$$

The boson-boson interaction and the bosonic tunnelling terms in $\hat{\mathcal{H}}$ and $\hat{\mathcal{H}}'$ act exactly in the same way over $|\Psi\rangle$ and $|\Psi\rangle'$. Also, one can easily convince itself that the fermionic tunnelling in $\hat{\mathcal{H}}$ acts over the fermion in $|\Psi\rangle$ in the same way as the same term in $\hat{\mathcal{H}}'$ does over the hole in $|\Psi\rangle'$. The only term that does not act in the same way in the two systems is the diagonal boson-fermion interaction. But the difference of eigenvalues for each of the Fock states with the same coefficient in $|\Psi\rangle$ and $|\Psi\rangle'$ is always $N_b U_{bf}$. For instance:

$$U_{bf}\sum_i \hat{a}_i^\dagger \hat{a}_i \hat{b}_i^\dagger \hat{b}_i \,|n_1,n_2,n_3;1,0,0\rangle = U_{bf} n_1 \,|n_1,n_2,n_3;1,0,0\rangle$$

and

$$\begin{aligned} &-U_{bf}\sum_i \hat{a}_i^\dagger \hat{a}_i \hat{b}_i^\dagger \hat{b}_i \,|n_1,n_2,n_3;0,1,1\rangle \\ &= -U_{bf}(n_2+n_3)\,|n_1,n_2,n_3;0,1,1\rangle \\ &= U_{bf}(n_1 - N_b)\,|n_1,n_2,n_3;0,1,1\rangle \end{aligned}$$

In Fig. 9 we show that our numerical results agree with the theoretical prediction that the spectra of the two systems should be shifted. Taking profit of this equivalence between the one and two-fermion systems, we shall study the two systems restricting ourselves to the case $U_{bb} > 0$, $U_{bf} < 0$, so that the case $U_{bb} > 0$, $U_{bf} > 0$ is also automatically examined for both systems.

Ground state and effect of the ratio $\Delta = \frac{|U_{bf}|}{U_{bb}}$

In principle, one would expect that the bosonic configuration of the one and two-fermion systems should be similar to one of the system with no fermions when the boson-boson and boson-fermion interaction strengths are the same, i.e., for $\Delta = 1$. However, in Figs. 10 and 11 one can see that this is not the case. As Λ is increased, not only the families of Mott-Insulator states of the one and two-fermion systems $\{|4,4,4;1,0,0\rangle\}$ and $\{|4,4,4;0,1,1\rangle\}$ have an important contribution to the ground state, but also the families of Fock states $\{|5,4,3;1,0,0\rangle\}$ and $\{|5,4,3;1,1,0\rangle\}$.

The reason for this difference can be explained on energetic grounds. In the systems with one and two fermions,

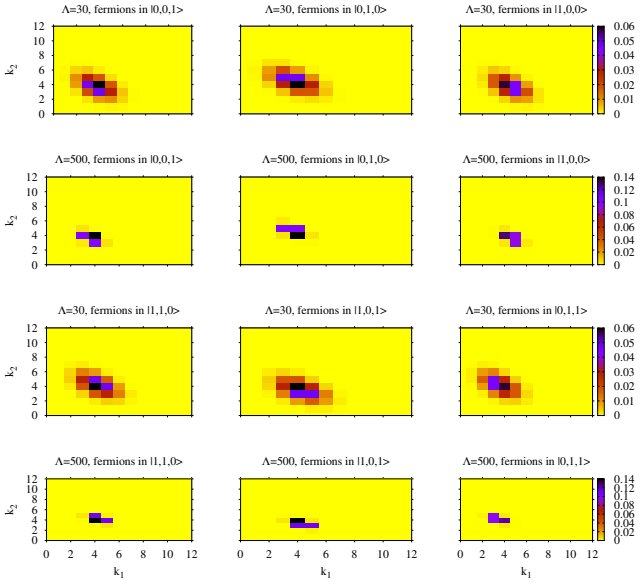

FIG. 10: Spectral decomposition $|c(k_1, k_2)|^2$ of the ground state of the one-fermion system (two upper rows) and the two-fermion system (two lower rows) for $\Delta = 1$ and $\Lambda = 30, 500$.

the expectation values of the Hamiltonian (1) over the Fock states are

$$\begin{aligned}&\frac{\langle n_1^b, n_2^b, n_3^b; n_1^f, n_2^f, n_3^f|\hat{\mathcal{H}}|n_1^b, n_2^b, n_3^b; n_1^f, n_2^f, n_3^f\rangle}{U_{bb}}\\&= \frac{1}{2}\left(n_1^b(n_1^b-1)+n_2^b(n_2^b-1)+n_3^b(n_3^b-1)\right)\\&-\Delta\left(n_1^b n_1^f + n_2^b n_2^f + n_3^b n_3^f\right).\end{aligned} \tag{17}$$

From (17), it is clear that the Fock states with a lowest expectation value of the energy depend on Δ. For the one-fermion system, these (families of) states are

$$\begin{aligned}&|4,4,4;1,0,0\rangle\,;\Delta\in[0,1)\\&|5,4,3;1,0,0\rangle\,;\Delta\in(1,2)\\&|6,3,3;1,0,0\rangle\,;\Delta\in(2,4)\\&|7,3,2;1,0,0\rangle\,;\Delta\in(4,5)\\&|8,2,2;1,0,0\rangle\,;\Delta\in(5,7)\\&|9,2,1;1,0,0\rangle\,;\Delta\in(7,8)\\&|10,1,1;1,0,0\rangle\,;\Delta\in(8,10)\\&|11,1,0;1,0,0\rangle\,;\Delta\in(10,11)\\&|12,0,0;1,0,0\rangle\,;\Delta\in(11,\infty)\end{aligned}$$
, (18)

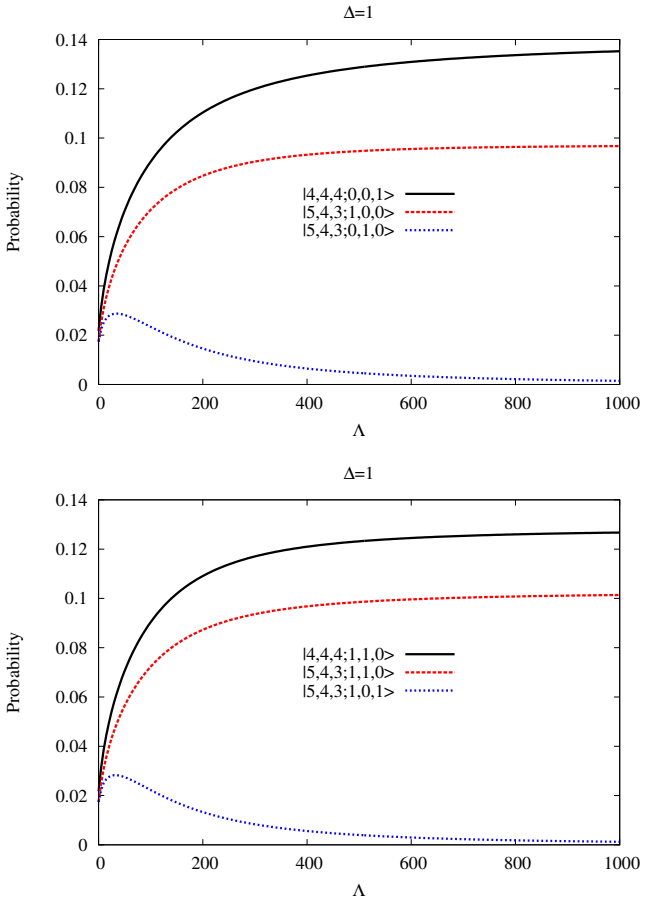

FIG. 11: Population of the lowest energy Fock states in the ground state of one- (upper panel) and two- (lower panel) fermion systems as a function of Λ. The Fock states obtained by permuting globally the bosons and fermions in the 3 sites are found in the ground state with the same probabilities.

, and for the two-fermion system

$$\begin{aligned}&|4,4,4;1,1,0\rangle\,;\Delta\in[0,1)\\&|5,4,3;1,1,0\rangle\,;\Delta\in(1,2)\\&|5,5,2;1,1,0\rangle\,;\Delta\in(2,4)\\&|6,5,1;1,1,0\rangle\,;\Delta\in(4,5)\\&|6,6,0;1,1,0\rangle\,;\Delta\in(5,\infty)\end{aligned}$$
. (19)

In the particular case $\Delta = 1$ shown in Figs. 10 and 11, both for the one and two-fermion systems, there are two families of Fock states with the lowest expectation value of the Hamiltonian, and this is why both of them have a significant presence in the ground state in the strongly interacting limit when the tunnelling between sites can be neglected. To reach the Mott-Insulator ground state in the strongly interacting limit, it is necessary to set $\Delta < 1$.

Possibly, the most interesting regime is that of high Δ ratio, when the relative strength of the boson-fermion at-

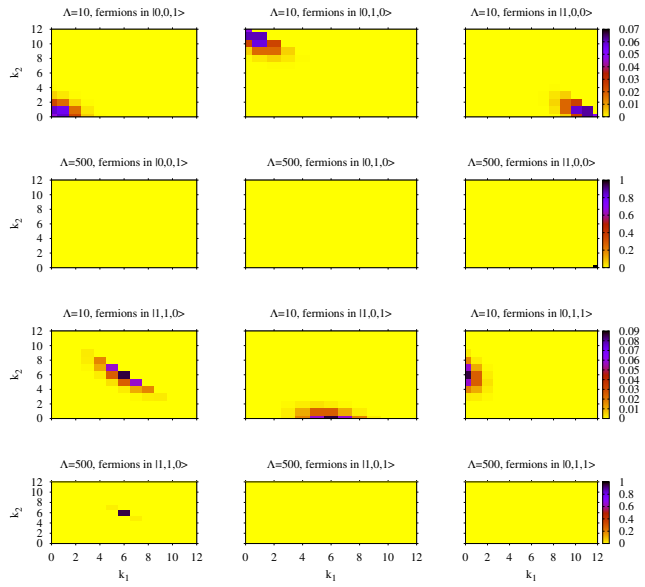

FIG. 12: Spectral decomposition $|c(k_1, k_2)|^2$ of the ground state of the one-fermion system (two upper rows) and the two-fermion system (two lower rows) for $\Delta = 14$ and $\Lambda = 10, 500$. Note that for $\Delta = 500$, the ground state of the one-fermion system essentially coincides with the Fock state $|12, 0, 0; 1, 0, 0\rangle$.

tractive interaction respect to the repulsive boson-boson interaction modifies dramatically the bosonic configuration: as can be seen in (11) and (12), the Fock states of least energy are those with a high number of bosons concentrated in the same site as a fermion instead of the states with the bosons spread in the 3 sites, as would be the case if there only was repulsive boson-boson interaction. This effect of concentration of the bosons is more important on the one-fermion system than in the two-fermion system because the bosons have fewer fermions with which interact and thus less sites to be spread in.

In order to have a better insight of this regime, we now set $\Delta = 14$, a value for which both in the one- and two-fermion systems the Fock state of least energy is as far from possible from the Mott-Insulator state, and study the properties of the ground states. In the non-interacting limit, the spectral decompositions of the two systems shown in Fig. 12 have the same density profile. In this limit, both ground states of the system are of mean-field type and can be found analytically

$$|\phi_0\rangle^{1\text{ fermion}}_{\Lambda=0} = \frac{\hat{b}_1^\dagger + \hat{b}_2^\dagger + \hat{b}_3^\dagger}{\sqrt{3N_b!}} \left(\frac{\hat{a}_1^\dagger + \hat{a}_2^\dagger + \hat{a}_3^\dagger}{\sqrt{3}}\right)^{N_b} |\text{vac}\rangle$$

$$|\phi_0\rangle^{2\text{ fermions}}_{\Lambda=0} = \frac{\hat{b}_1^\dagger\hat{b}_2^\dagger + \hat{b}_2^\dagger\hat{b}_3^\dagger + \hat{b}_1^\dagger\hat{b}_3^\dagger}{\sqrt{3N_b!}} \left(\frac{\hat{a}_1^\dagger + \hat{a}_2^\dagger + \hat{a}_3^\dagger}{\sqrt{3}}\right)^{N_b} |\text{vac}\rangle\,. \tag{20}$$

These two ground states have the same bosonic configurations, and the fermionic configurations are equivalent under a particle-hole transformation (in the one-fermion system the fermion is completely delocalized and in the two-fermion system the hole is completely delocalized).

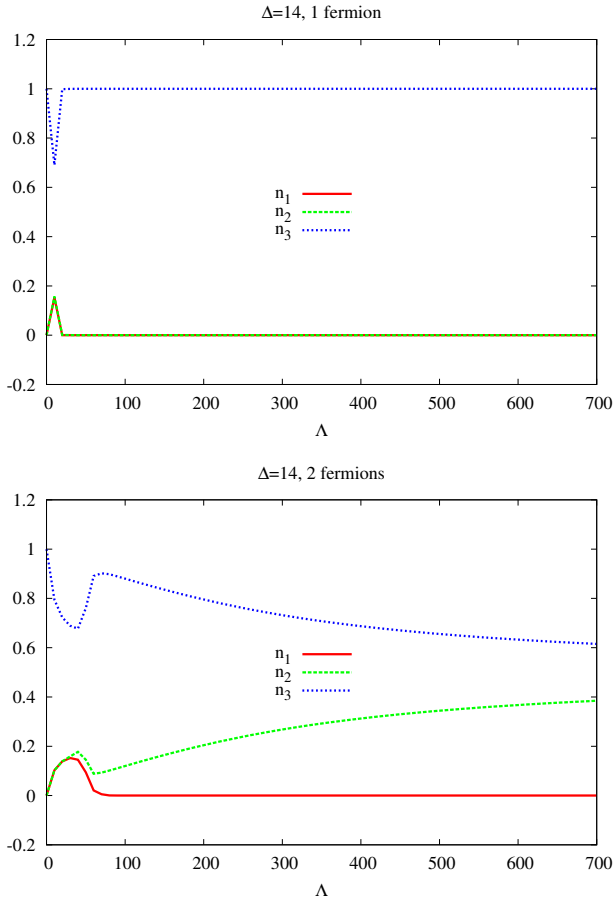

FIG. 13: Eigenvalues of the bosonic one-body density matrix (divided by $N_b = 12$) of the one-fermion (top) and two-fermion (bottom) systems, for $\Delta = 14$, as a function of the interaction strength Λ.

Contrary to what happened in the case $\Delta = 1$ shown in Figs. 10 and 11, when the interaction is turned on the spectral decompositions of the ground state of the one and two fermion systems show very different bosonic configurations even at low values of Λ. This is due to the fact that the boson-fermion interaction causes the Fock states of lower energy to be different in the two systems, and these are the states that start becoming more populated when the interaction strength is increased. In the limit of very strong interaction, the one-fermion ground state essentially coincides with the Fock state $|12, 0, 0; 1, 0, 0\rangle$ and the two-fermion ground state with the Fock state $|6, 6, 0; 1, 1, 0\rangle$. Other states equivalent under global permutations of bosons and fermions do not appear due to the bias introduced in the Hamiltonian. The eigenvalues of the bosonic one-body density matrix plotted in Fig. 13 also show a different behavior as a function of the interaction strength for the one and two-fermion sys-

tems. In both cases, at $\Lambda = 0$ there is an eigenvalue $N_b n_3$ of the bosonic one-body density matrix which is equal to the total number of bosons. This is due to the fact that in this limit the ground state of both systems can be written as a mean-field state (20). In the case of the one-fermion system, as Λ is increased $N_b n_3$ decreases, but eventually it increases again and goes to the total number of bosons: the interaction strength is high enough that the tunnelling term can be neglected and the ground state essentially coincides with the Fock state $|12, 0, 0; 1, 0, 0\rangle$, where all the bosons are in the same site and thus fully condensed. The eigenvalues in the two-fermion system undergo a similar decreasing behavior as in the one-fermion system on the first place. Then, $N_b n_3$ increases again, but eventually reaches a maximum and then decreases monotonically. Thus, the bosons are never fully condensed expect for the special case $\Lambda = 0$. In the strongly interacting limit, two of the eigenvalues go to 6 and the third to 0, consistently with the fact that the ground state essentially coincides with the Fock state $|6, 6, 0; 1, 1, 0\rangle$.

In both systems, the fact that the boson-fermion interaction strength is much higher than the boson-boson modifies the condensation properties of the bosons in the absence of fermions (Fig. 8), and in the case of the one-fermion system it is even capable to induce full condensation in a bosonic system which without the fermion would be completely delocalized.

IV. CONCLUSIONS

We have used exact diagonalization methods to study the effect of the interaction of few fermions with a background of bosons in few-site systems described through a Hubbard type Hamiltonian.

First, we have studied the case of a two-site system with a single fermionic impurity. Already in this simple case, the interaction with the impurity induces quantum correlations that modify the properties of the ground state. We have also shown that these correlations are present in the dynamic evolution of the system.

In order to spot some genuine effect of the Fermi-Dirac statistics, we have next considered a three-site system, in which a maximum of three fermions can be hosted. We have shown that in the case of boson-fermion interactions stronger than boson-boson interactions, the ground state properties of the bosons are drastically modified by the presence of the fermions. We have also shown that these effects are different when there are two fermions in the system than when there is only one.

However, in the three-site system it is possible to map the one- and two-fermion systems by switching the sign of the boson-fermion interaction, so one could argue that not even in this system genuine effects of the fermionic nature of the impurities can arise. Thus, an interesting and computationally challenging starting point for further research would be to increase the number of sites in the system so that more fermions can be placed in it.

Acknowledgments

I specially want to acknowledge my advisors Bruno Juliá-Díaz and Artur Polls for their continuous guidance and help in this project. I would also like to thank my family and friends for their support and encouragement.

[1] S. Will, PhD Thesis (2011). *Interacting bosons and fermions in three-dimensional optical lattice potentials: From atom optics to quantum simulation.* Johannes Gutenberg-Universität, Mainz, Germany.

[2] K.J. Günter, PhD Thesis (2007). *Interacting Fermi gases and Bose-Fermi mixtures in optical lattices.* Swiss Federal Institute of Technology, Zurich, Switzerland.

[3] C. Chin, R. Grimm, P. Julienne, and E. Tiesinga, Rev. Mod. Phys. **82**, 1225 (2010).

[4] M. Lewenstein, A. Sanpera and V. Ahufinger, *Ultracold atoms in optical lattices. Simulating quantum many-body systems.* (Oxford University Press, Oxford, 2012).

[5] N.J.S. Loft, A.S. Dehkharghani, N.P. Mehta, A.G. Volosniev and N. T. Zinner, European Physical Journal D, 69, 65 (2015).

[6] A.G. Volosniev, D.V. Fedorov, A.S. Jensen, M. Valiente and N.T. Zinner, Nature Communications **5**, 5300 (2014).

[7] G.E. Astrakharchik and I. Brouzos, Physical Review A **88**, 021602(R) (2013).

[8] T. Sowiński, T. Grass, O. Dutta, and M. Lewenstein, Physical Review A **88**, 033607 (2013).

[9] M.A. García-March, B. Juliá-Díaz, G.E. Astrakharchik, J. Boronat, and A. Polls, Physical Review A **90**, 063605 (2014).

[10] H. Fehrmann, M.A. Baranov, B. Damski, M. Lewenstein and L. Santos, Optics Communications 243, 2331 (2004).

[11] F. Illuminati and A. Albus, Phys. Rev. Lett. **93**, 090406 (2004).

[12] L.D. Carr and M.J. Holland, Physical Review A **72**, 031604(R) (2005).

[13] H. Frahm and G. Palacios, Physical Review A **72**, 061604(R) (2005).

[14] B. Juliá-Díaz, D. Dagnino, M. Lewenstein, J. Martorell and A. Polls, Phys. Rev. A **81**, 023615 (2010).